Structural elements on reconstructed Si and Ge(110) surfaces

A. A. Stekolnikov, J. Furthmüller, and F. Bechstedt
Institut für Festkörpertheorie und Theoretische Optik, Friedrich-Schiller-Universität, Max-Wien-Platz 1, 07743 Jena, Germany
(Received 2 December 2003; published 7 July 2004)

We present *ab initio* studies of possible reconstruction elements on Si and Ge(110) surfaces. Using 2×2, 3×2, and 6×2 unit cells we optimize models with buckled atomic chains, dimers, different adatom distributions, and interstitial atoms which may exist on the larger Si(110)16×2 or Ge(110)$16\times2/c(8\times10)$ surface reconstructions. We show that adatom reconstructions gain energy. Only the adatom model which seemingly leaves no dangling bonds cannot occur on Si and Ge(110) surfaces. An adatom-rest atom electron transfer mechanism is more favorable. An adatom-tetramer-interstitial 3×2 model also stabilizes the Si and Ge surfaces and leads to a semiconducting behavior (at least for Si). Simulated scanning tunneling microscopy (STM) images of empty states of this reconstruction look like the pentagon structures observed on Si(110)16×2. A 6×2 reconstruction with five-membered adclusters is energetically completely unfavorable, though it also reproduces the empty-state pentagonlike STM images.

DOI: 10.1103/PhysRevB.70.045305 PACS number(s): 68.35.Bs, 68.35.Md, 73.20.At

I. INTRODUCTION

Among the low-index silicon (Si) and germanium (Ge) surfaces, the (110) surfaces are the only ones whose atomic structures are still unknown. At least for silicon, the (110) surface has a free energy only slightly larger than that of the (111) plane.[1] It should therefore be a stable facet of the equilibrium crystal shape.[2] However, the preparation of such surfaces is difficult. Only nonvicinal, clean and well annealed Si(110) surfaces exhibit a 16×2 reconstruction (Wood notation) or, more precisely, a

$$\begin{pmatrix} 11 & -5 \\ 2 & 2 \end{pmatrix}$$

reconstruction within the matrix notation.[3–6] Contaminations, for example very small amounts of Ni, destroy the long-range reconstruction and give rise to translational lattices with smaller unit cells, e.g. 5×1.[3,7,8] Scanning tunneling microscopy (STM) experiments[3,5,6] suggest that the Si(110)16×2 reconstruction consists of equally spaced and alternately raised and lowered stripes lying along the $[1\bar{1}2]$ direction. The height of the steps between two stripes is equal to the layer spacing in normal direction. Along the stripes these experiments reveal arrangement of "pairs of pentagons" which are more pronounced in empty-state images.[6] The experimental situation is less clear for the Ge(110) surfaces. In the pioneer work Olshanetsky *et al.*[9] it was shown that a $c(8\times10)$ superstructure appears after annealing. Despite the existence of STM images for Ge(110)$c(8\times10)$,[10] there are indications that the $c(8\times10)$ structure is transient and unstable and changes into a 16×2 superstructure.[11,12] However, for both periodicities the STM images show sequences of pentagons similar to the findings for the Si(110) surface.

There are no accepted structural models for the reconstructed Si and Ge(110) surfaces which consistently explain the energetics, the geometry and the electronic structure, in particular the STM images. Usually a certain distribution of adatoms and several top layers involved in the reconstruction are assumed to interpret the atomic structures of Si(110)16×2 (Refs. [4,6,13,14]) and Ge(110)$c(8\times10)$ (Ref. [10]) or 16×2 (Refs. [11,12]) unit cells. Conglomerates of adatoms which capture interstitial atoms such as in the case of Si(113) surfaces[15] have been suggested by An *et al.*[6] to explain the pentagon pairs observed in high-resolution STM images of the Si(110)16×2 surface. The origin of the stabilization of Ge(110) surfaces by certain reconstruction elements is also not understood. Recently, Ichikawa[12] explained the STM images observed for the Ge(110)16×2 surface by pairs of five-membered adclusters. However, such structures are questionable from the energetical point of view.

Apart from one trial[12] theoretical studies have not been performed for the large 16×2 or $c(8\times10)$ unit cells. Some attempts were devoted to find favorable reconstruction elements and to understand the bonding behavior by studying smaller unit cells.[13,16–18] In particular, it has been found that a bond-rotation relaxation mechanism should take place on Si and Ge(110) surfaces[16–18] where the top-layer atomic chains are buckled like in the case of III-V compounds.[2] Dimerization similar to the (100) case has been proposed based on tight-binding (TB) calculations.[13] Possible structures with adatoms have been studied by means of both *ab initio*[17] and TB molecular-dynamics calculations.[16] The suggestion of fully bonded (i.e., fourfold-coordinated) adatoms which leave no dangling bonds[16,17] is rather surprising for group IV semiconductor surfaces and needs additional studies.

In this paper we present first-principles studies of energetical and structural properties of possible reconstruction elements on Si and Ge(110) surfaces. The electronic structures accompanying the most stable reconstructions are studied to understand the mechanisms of surface stabilization. We focus on models including chains with rotated and contracted bonds, adatoms in different sites, and interstitial atoms in unit cells of surfaces with 1×1, 1×2, 2×1, $c(2\times2)$, 2×2, 3×1, 3×2, and 6×2 translational symmetry. STM images of the models with adatom-tetramer-interstitial elements or five-membered adclusters are simu-

lated to explain perhaps the pentagonal structure elements. Finally, we present a possible model for Si and Ge(110)16 $\times 2$ reconstructions.

II. COMPUTATIONAL DETAILS

Our calculations are performed within the density-functional theory[19] (DFT) in the local-density approximation (LDA).[20] The electron-electron interaction is described by the Ceperley-Alder functional as parameterized by Perdew and Zunger.[21] The interaction of the electrons with the atomic cores is treated by non-normconserving *ab initio* ultrasoft pseudopotentials.[22] Nonlinear core corrections are also taken into account.[23] Explicitly we use the VASP code.[24] In the bulk case the DFT-LDA yields cubic lattice constants of $a_0=5.398$ and 5.627 Å and indirect fundamental energy gaps $E_g=0.46$ and 0.00 eV for Si and Ge, respectively. Quasiparticle corrections[25,26] are not added to the Kohn-Sham eigenvalues[20] of the DFT-LDA in order to take into account the excitation aspect.

In the cases of 1×2, 2×1, and $c(2\times2)$ reconstructions lateral 2×2 unit cells are used to minimize the total energy. For the variety of 3×1 and 3×2 reconstructions 3×2 unit cells are studied. The surfaces are modeled by repeated slabs. Each 2×2 slab consists of 11 atomic layers and the same amount of vacuum layers. For 3×2 and 6×2 cells 7 atomic layers and 9 layers of vacuum are used. The bottom sides of the slabs are passivated by hydrogen atoms and kept frozen during the surface optimization. The topmost eight or five layers of the slabs with 2×2 or 3×2 and 6×2 lateral cells are allowed to relax. Six, four or two **k** points are used in the irreducible part of the Brillouin zone (BZ) for surfaces with 2×2, 3×2 or 6×2 translational symmetry. A surface geometry is determined by allowing the atomic positions to relax until the Hellmann-Feynman forces are smaller than 10 meV/Å. The eigenvalues and eigenfunctions of the Kohn-Sham equation[20] are used to calculate the local electronic density of states and the STM images within the Tersoff-Hamann approach.[27] A constant-height mode is assumed for the STM simulations.

III. RESULTS AND DISCUSSION

The studied most important surface reconstructions are shown in Fig. 1. Resulting surface energies are given in Table I.

A 1×1 unit cell of (110) surfaces consists of two atoms with one dangling bond at each atom. After the relaxation these atoms possess asymmetric positions, one atom goes up while the other one moves down, thereby introducing a buckled chain. Additionally the atoms can be somewhat twisted along the chain direction. In the case of III-V semiconductors the (110) surface is the cleavage face.[2] Because of the electrostatic neutrality of a surface unit cell, only such a bond-rotation or a bond-contraction relaxation occurs. The dangling bond of the upper atom (the cation) is completely filled with electrons while that of the lower atom (the anion) gets empty. However, a 1×1 reconstruction with a bond-rotation or bond-contraction-relaxation mechanism is not the most favorable one for Si and Ge(110) surfaces. A more stable reconstruction with parallel chains buckled in opposite directions is presented in Fig. 1(a). The lateral displacements of the first layer atoms nearly guarantee the bond-length conservation. This 1×2 reconstruction is energetically more favorable than the relaxed 1×1 one for both materials. The energy gains due to the various buckling contributions of the chains are only of the order of 10 meV for Si and slightly larger for Ge (about 20 meV). The stabilization by antiphase chains agrees with previous theoretical findings.[16,17] The values of the buckling amplitudes are 0.75 and 0.80 Å for Si and Ge, respectively. The preference of the 1×2 reconstruction can be related to a gain of band-structure energy. The corresponding electronic band structures are plotted in Fig. 2(a). In contrast to the findings for the relaxed 1×1 surface,[18] the alternate buckling of parallel chains in the 1×2 reconstruction opens a fundamental band gap between

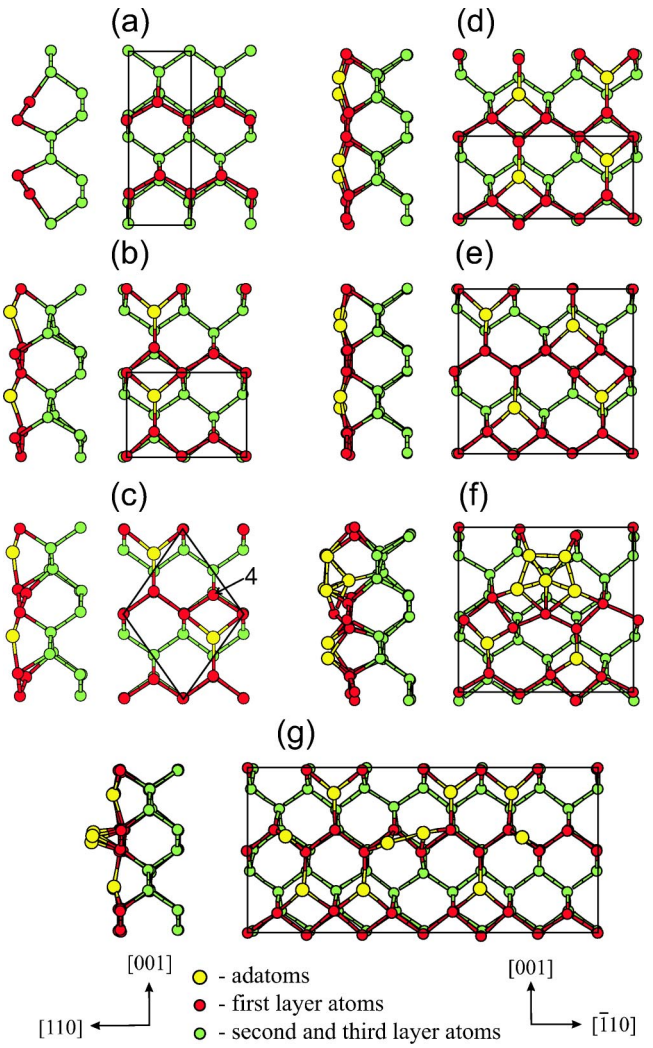

FIG. 1. (Color online) Side and top views of relaxed atomic positions of Si(110) surfaces (those for Ge are similar): (a) 1×2 chain buckled model, (b) 2×1 adatom model, (c) $c(2\times2)$ adatom model, (d) 3×1 adatom model, (e) 3×2 adatom model, (f) 3×2 adatom-tetramer-interstitial model, and (g) 6×2 five-membered adatom model. Lateral unit cells are indicated by thin solid lines in the top views.

TABLE I. Reconstruction-induced energy gain per 1×1 unit cell in eV with respect to the bulk-terminated (i.e., unrelaxed 1×1) surface. Results for bond-length-conserving chain 1×1 and 1×2 reconstructions, adatom models with 2×1, $c(2\times2)$, 3×1, or 3×2 translational symmetry, an adatom-tetramer-interstitial (ATI) 3×2 geometry, and a 6×2 five-membered cluster reconstruction are presented.

Reconstruction	ΔE_{surf}(eV/1×1 cell)	
1×1	0.44	0.47
1×2	0.45	0.49
2×1-adatom	0.49	0.53
$c(2\times2)$	0.37	0.29
3×1	0.54	0.41
3×2	0.40	0.32
3×2-ATI	0.54	0.52
6×2	≈0	≈0

surface bands. For Si a small gap is observed along the $J'K$ direction. The interchain interaction is effectively reduced. The band folding together with the repulsion of bands decrease the band dispersion in chain direction. For Ge the band structure in Fig. 2(a) indicates a metallic behavior. However, the interpretation of the Ge electronic states is more difficult because of the underestimation of the band gaps within the DFT-LDA already for bulk, in particular the zero fundamental gap. The dispersion of the surface bands in Fig. 2(a) is not too large, and the bands mostly overlap near the Γ point. There may be a chance to open a gap using the quasiparticle approach.[25,26] This also holds for other Ge surface reconstructions discussed below. In contrast to the Ge case the Si(110)1×2 surface with oppositely buckled parallel chains is semiconducting. The dispersion of the surface bands near Γ is much weaker. For Si(110)1×2 the squares of the wave functions at K are shown for the highest occupied and lowest unoccupied states in Fig. 3. The principal behavior is similar to the case of equally buckled chains in 1×1 cells. The states localized on upper atoms are fully occupied and behave as s-like orbitals, while those on lower atoms are empty and have p_z-like character. The surface states are similar for Ge (not shown).

Another 1×2 reconstruction may be related to a phase-shifted arrangement of π-bonded dimers,[13] due to the rebonding of dangling bonds of neighboring first-layer atoms belonging to the same chain along the $[1\bar{1}0]$ direction (not shown in Fig. 1). The total-energy optimization showed that such dimer arrangements are not stable. During the atomic relaxation the starting dimer configuration is transformed back into a chain structure. The reason is that it is not favorable to break a σ bond which already exists and create a dimer with a π bond which is weaker. Consequently, it is not possible to cover Si and Ge(110) surfaces by neighboring dimers.

Other important reconstruction elements contain adatoms in different positions in order to reduce widely the number of dangling bonds. We have studied a variety of reconstruction models with adatoms. The most favorable (for Ge) and energetically second (for Si) adatom reconstruction leads to the 2×1 surface shown in Fig. 1(b). One adatom on a 2×1 cell saturates three dangling bonds of first-layer atoms. The remaining dangling bond belongs to a rest atom. One expects an energy gain due to an adatom-rest atom mechanism,[2] such as occurs on a Ge(111)$c(2\times8)$ surface.[18] Indeed, the 2×1 adatom model in Fig. 1(b) further lowers the surface energy (see Table I) for both Si and Ge(110) surfaces. However, the energy gain is much smaller than that computed by Takeuchi.[17] The adatom-rest atom mechanism determines the surface electronic structure. This is clearly indicated in Fig. 2(b). The calculated band structures exhibit the opening of a band gap, at least in the case of Si. A nearly direct band gap occurs at the J point. In the Ge case surface bands overlap with bulk states near Γ. The squares of the surface wave functions at K are presented in Fig. 4 for Si. The localization of the wave functions and the state occupation confirm the classical picture of an adatom-rest atom charge transfer. The occupied states with s-like character are observed at the rest atoms which are displaced from the surface towards the vacuum region. The dangling bond of the adatom is more

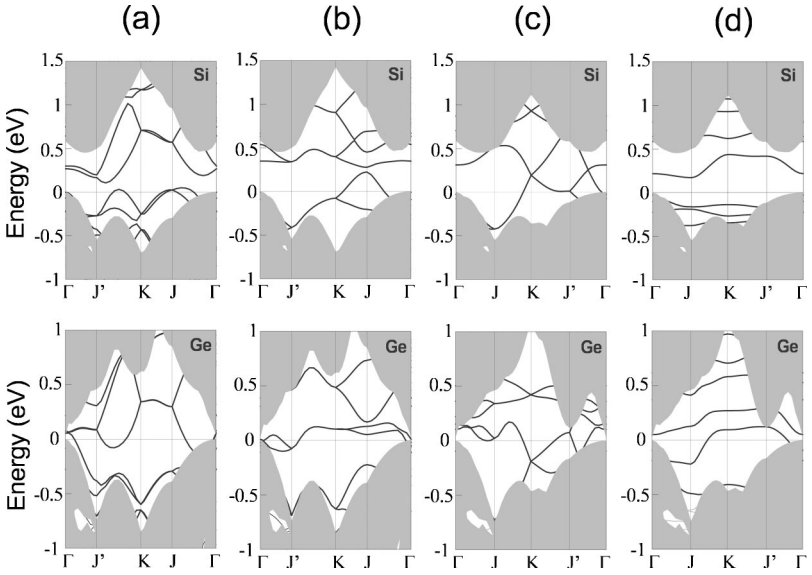

FIG. 2. Band structures of Si and Ge(110) surfaces. (a) 1×2 with oppositely buckled chains, (b) 2×1 adatom model, (c) 3×1 adatom model, and (d) 3×2 adatom-tetramer-interstitial model. The Brillouin zone of the 2×2 (3×2) structure is used to present the bands obtained for 1×2, 2×1 (3×1, 3×2) translational symmetry.

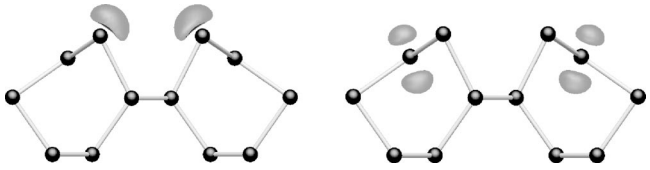

FIG. 3. Wave-function squares at K for the Si(110)1×2 surface with oppositely buckled chains. Left panel: highest occupied state; right panel: lowest unoccupied state.

p_z-like. Consequently, more or less one electron is transferred from the adatom to the rest atom. The same tendency is observed for Ge. The vertical differences between adatom and rest atom positions are rather small with 0.31 and 0.26 Å for Si and Ge, respectively.

One attempt to accommodate adatoms in appropriate distances and to saturate all dangling bonds is shown in Fig. 1(c). According to a common believe one adatom on a $c(2\times2)$ unit cell should allow an arrangement with a complete saturation of the dangling bonds. According to Ref. 17 the adatom is bonded to four different atoms in neighbored chains. Bonds with lengths of 2.4 and 2.6 Å should give rise to an extremely large energy gain of more than 1 eV/1×1 cell. The results of the careful relaxation of the structure in Fig. 1(c) indicate a completely different behavior. The energy gain in Table I is much smaller; smaller than those of all bond-length-conserving chain reconstructions [e.g. that shown in Fig. 1(a)] and the 2×1 adatom model. The structural data are in agreement with the energetical findings. We derive a much larger distance between the adatom and the fourth (most distant) atom that contributes to the seemingly fourfold coordination of the adatom. The different results (with respect to Ref. 17) can be related to a better convergence concerning the number of atomic layers in the slab, the BZ sampling, and the energy cutoff of the plane-wave expansion. The critical distance between adatom and fourth atom amounts to 2.87 (3.08) Å for Si(Ge), i.e., in between $a_0/2$ and $\sqrt{3/2}(a_0/2)$. This value is much larger than the characteristic bond length 2.34 (2.44) Å and can be only related to an extremely weak bond. The physical/chemical reasons for the findings are obvious. Si and Ge atoms prefer fourfold coordination with tetrahedral bonding. An arrangement of four nearest neighbors in nearly one plane is rather unfavorable. An adatom with a p_z-like dangling orbital can only have a weak overlap with the dangling bond at the fourth atom. Another configuration with a stronger wavefunction overlap would however induce a remarkable strain in the atomic layers below. The situation is similar to the case of adatoms on Si and Ge(111) surfaces[2] or to the 2×1 adatom reconstruction discussed above. The resulting geometry allows for another interpretation. The adatom and the fourth atom, the chain atom in [001] direction with a remaining dangling bond, represent an adatom-rest atom pair but not a pair with true bonding.

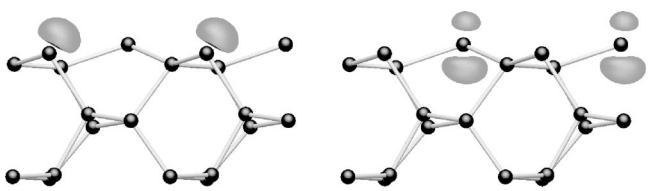

FIG. 4. Wave-function squares at K for the adatom model of the Si(110)2×1 surface. Left panel: highest occupied state, right panel: lowest unoccupied state.

Using 3×1 and 3×2 unit cells we have optimized structures where all dangling bonds of the original (110) surfaces are saturated by adatoms. Such 3×1 and 3×2 reconstructions are shown in Figs. 1(d) and 1(e), respectively. Each adatom is threefold coordinated. There remains only one dangling bond per adatom. The adatom reconstruction models substantially reduce the dangling bond density, the number of dangling bonds per 1×1 unit cell. Instead of 2 in the 1×2 case with buckled chains or 1 for the 2×1 and $c(2\times2)$ adatom models the dangling bond density is further reduced to 2/3. However, in contrast to the other adatom reconstructions no rest atoms occur. The distribution of the adatoms in the 3×2 structure (i.e., pair of adatoms) looks similar to the reconstruction element suggested as a building block for the unit cell of the Si(110)16×2 surface.[4,28] The 3×1 arrangement of the adatoms following each other in [001] direction [Fig. 1(d)] is more favorable from the energetical point of view for Si (see Table I). In the Ge case it is less favorable than the 2×1 adatom reconstruction. These contradictory findings are similar to those for the (111) surfaces, where the adatom-rest atom pairs on $c(2\times8)$ cells are the most favorable reconstruction elements for Ge but not for Si.[18] Surprisingly, the out-of-phase arrangement of the adatoms within the 3×2 translational symmetry [Fig. 1(e)] is much higher in energy (cf. Table I). This fact confirms that Si and Ge(110) surfaces are "sensitive" with respect to the adatom distributions. To reduce probably the surface stress we also have tested a structure with two adatom-rest atom pairs but in 2×2 unit cells (not shown in Fig. 1). It gains 20 meV per 1×1 cell for Si and 50 meV in the case of Ge in comparison with the 3×2 periodicity. However, in both cases the values lie quite far from those for the most favorable adatom reconstructions.

The general weak tendency for a stabilization of a pure adatom structure is understandable because of the nearly identical bonding behavior of the adatoms and the resulting bands. It is accompanied with metallic band structures as indicated in Fig. 3(c) for both Si and Ge(110)3×1 adatom structures. The low surface energy of the Si(110)3×1 adatom reconstruction and its metallic band structure do not contradict the reconstruction rules for semiconductor surfaces.[2] Similar observations have been made for other surface orientations. The Si(111)7×7 surface possesses a metallic band structure but is the energetically most favorable reconstruction. In the Ge(111) case the lowest-energy structure $c(2\times8)$ is semiconducting. This is in agreement with the fact that the Ge(110)2×1 adatom reconstruction is also the lowest one in energy (see Table I).

Based on the idea to explain the STM findings for Si(110)16×2 surfaces by pentagons which are formed by tetramer and interstitial atoms,[6] we have studied such reconstruction elements in 3×2 unit cells. We followed the ideas developed to interpret the 3×2 reconstruction of Si and

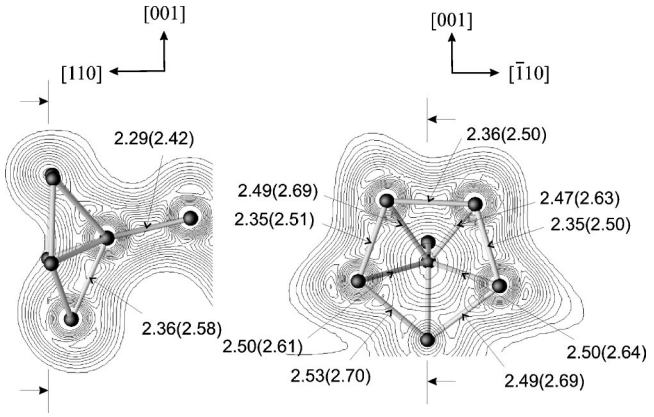

FIG. 5. Charge density plot around the interstitial and pentamer atoms for the 3×2 adatom-tetramer-interstitial reconstruction of Si(110). Planes used for representation are indicated by arrows. Bonds lengths are also given for Ge (in brackets)

Ge(113) surfaces by adatom-dimer-interstitial (ADI) and adatom-interstitial (AI) models.[29] The pentagon (or pentamer) in one half of a 3×2 cell consists of four adatoms (tetramer) and one atom belonging to a chain in the first atomic layer. They saturate five of the six surface dangling bonds. The interstitial atom is laterally located at the center of the pentamer but below the pentamer plane. In the second half of the 3×2 cell two additional adatoms saturate the dangling bonds in such a way that one rest atom is left. The resulting 3×2 adatom-tetramer-interstitial (ATI) reconstruction is drawn in Fig. 1(f). The total-energy minimizations show that the ATI reconstruction is the same in energy with respect to the most favorable 3×1 adatom Si structure. For Ge the energy gain is also comparable to that calculated for the 2×1 adatom reconstruction. We optimized structures where pentamers have no subsurface interstitial atoms. These reconstructions have been found less favorable. However, the reconstruction with a pentamer and an interstitial atom gains energy only in combination with two adatoms, at least within the 3×2 translational symmetry. For Si the energy difference between the models with and without additional adatoms amounts to 0.21 eV per 1×1 unit cell. The reason will be discussed below describing the band structure.

The interstitial atom is sixfold coordinated. In Fig. 5 the strength of the bonds between this atom and its neighbors is discussed in terms of the bond lengths and the electron distribution. The side view in Fig. 5 clearly indicates that the interstitial atom creates a strong bond with the atom below in the second-atomic layer. The shortest bond of 2.36 (2.58) Å with the fifths pentamer atom is strong (weak) for Si (Ge). The bonds to the other four pentamer atoms are usually weaker with lengths of about 2.5 (2.6–2.7) Å. At least for Si, three (of five) strong bonds between pentamer atoms are indicated by keeping nearly the bulk bond length. This is also clearly indicated by the electron distribution between the pentamer atoms. The two bonds with the fifth pentamer atom (i.e., a chain atom in the first atomic layer) are weaker. This is a consequence of the fact that this atom has five nearest neighbors [cf. Fig. 1(f)]. The four adatoms of the pentagon are fourfold coordinated. However, they do not anymore show a sp^3 hybridization.

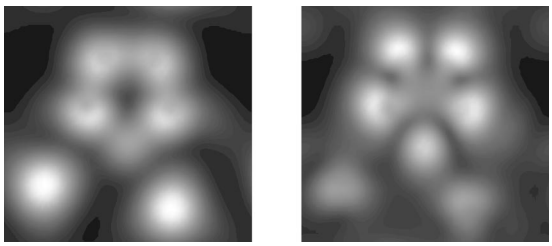

FIG. 6. Simulated STM images of filled (left panel) and empty (right panel) states of the 3×2 adatom-tetramer-interstitial Si(110) surface for bias voltages corresponding to −2 and 2 eV with respect to the theoretical Fermi level.

An indication for the large energy gains arises from the band structures in Fig. 2(d). There is a tendency for opening of an energy gap between the surface-state bands. The gap of the 3×2 ATI reconstruction is the largest one among all studied Si(110) reconstructions. The opening mechanism is similar to that discussed for the Si(113)3×2 ADI surface.[29] Due to the weak bonding pentamer atoms donate electrons to the two adatoms in the second half of the 3×2 unit cell. Their dangling bonds are fully occupied with electrons which form lone pairs. As a consequence the filled-state (empty-state) STM images are dominated by adatom (pentamer-atom) electronic states. This is demonstrated in Fig. 6. For the Si(110)3×2 ATI surface the STM images simulated for a bias of −2 V (2 V) mainly show the adatoms (pentamer atoms) in the lower (upper) half of the 3×2 surface unit cell. The STM image simulated for the empty states seems to be similar to the characteristic pentagon-shaped element of the empty-state STM images observed for the Si(110)16×2 surface.[6]

We have also optimized a 6×2 reconstructed geometry which consists of two five-membered adclusters as proposed in Ref. 12 for the Ge(110)16×2 surface. Its structure is presented in Fig. 1(g). Each of the clusters has three adatoms and two bridge-site atoms. Two bridge-site atoms belonging to different adclusters form a bond between each other.[12] Along the chain direction in the underlying atomic layer clusters are separated by four atoms at nearly ideal positions. However, the above described structure is not stable for both Si and Ge. We could not really find local minima on the total-energy surfaces. The atomic forces remain too large. In contrast to Ref. 12 in our calculations the convergence criterion concerning the forces is stronger by one order of magnitude. The reason of the structural instability could be an oversaturation of surface bonds. Two adatoms along the chain in each cluster are located in such a way that they seemingly saturate the dangling bonds of one atom twice. Additionally the two bridge-site atoms weaken a σ chain bond and give rise to four new bonds. Consequently, depending on the starting configuration a bridge-site atom may saturate a dangling bond of the next chain atom or a neighboring adatom.

Simulated STM images of the Ge(110)16×2 reconstruction with five-membered clusters look similar to the images observed experimentally.[12] This similarity was interpreted as a proof for the existence of the assumed reconstruction element. Our calculated STM images are presented in Fig. 7 for

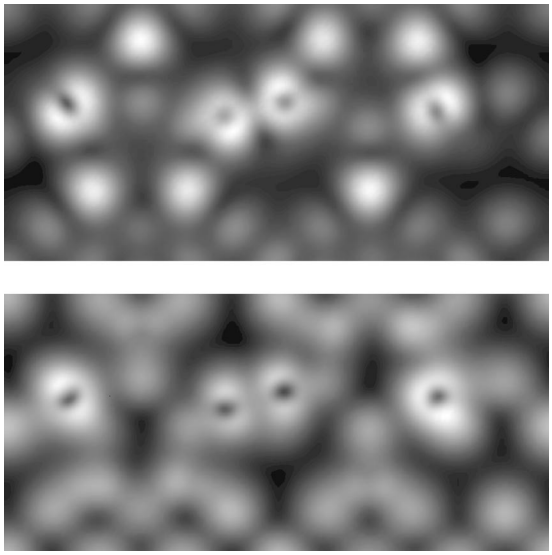

FIG. 7. Simulated STM images of empty (top panel) and filled (bottom panel) states of the 6×2 five-membered clusters Si(110) surface for bias voltages corresponding to 2 and −2 eV with respect to the theoretical Fermi level.

the Si(110)6×2 reconstruction. We note, that the adatoms of the 6×2 reconstruction model take remarkably different vertical positions [cf. Fig. 1(g)] and, hence, make it difficult to choose an appropriate plane to compute the constant-height STM images. Moreover, the comparison of the images obtained in constant-height mode with measured constant-current mode images is rather problematic. We use a plane which crosses the bridge-site atoms. The calculated empty-state images in Fig. 7 (top panel) for Si show spot arrangements similar to the observed pentagon-shaped ones. States originating from all adcluster atoms including the bridge-site atoms contribute to the empty-state image of the 6×2 reconstruction. In contrast, in Fig. 7 (bottom panel) occupied states give only contributions at bridge-site atoms and not at the other adatoms. We have also not found any contribution of occupied states which are located at adatoms using a three-dimensional representation of the wave functions. If the plane to plot the constant-height STM images is closer to the surface, it is, however, more probable to see states localized at the four rest atoms belonging to the chain. In general, it is not possible to observe significant pentagon structures in both empty and occupied images for the described 6×2 reconstruction.

Following the results obtained for the energetics of the reconstruction elements on (110) surfaces we have to conclude that for both materials, Si and Ge, the adatom-tetramer-interstitial model in Fig. 1(f) should describe an important element of the 16×2 reconstruction, if it actually represents an equilibrium surface phase and is not influenced by kinetic effects or sample preparation. In particular in the Ge case it should be combined by a preferential arrangement of adatoms along the [001] direction [see Fig. 1(b)]. Of course, the pentagons have to be arranged in zigzag lines along the $[\bar{1}12]$ direction, in order to account for the corresponding stripes found in STM images.[6] In addition, a reasonable reconstruction model of the $(110)16\times2$ surfaces of Si and Ge should also include monolayer steps accompanied by the formation of trenches along $[\bar{1}12]$ with a width of half of the 16×2 unit cell as observed by STM.[4,6] A possible resulting reconstruction model is presented in Fig. 8. A certain rebonding across the steps has been assumed. However, the shape of the steps and the probably accompanying energy gain have to be proved in future total-energy calculations. The zigzag chains of pentagon-shaped elements parallel to the steps and the additional adatoms are arranged in lines parallel to [001]. According to STM images of the isolated reconstruction elements in Fig. 6 we expect that their zigzag arrangements in the model of Fig. 8 may reproduce the stripes on lower and higher terraces seen in the STM images.

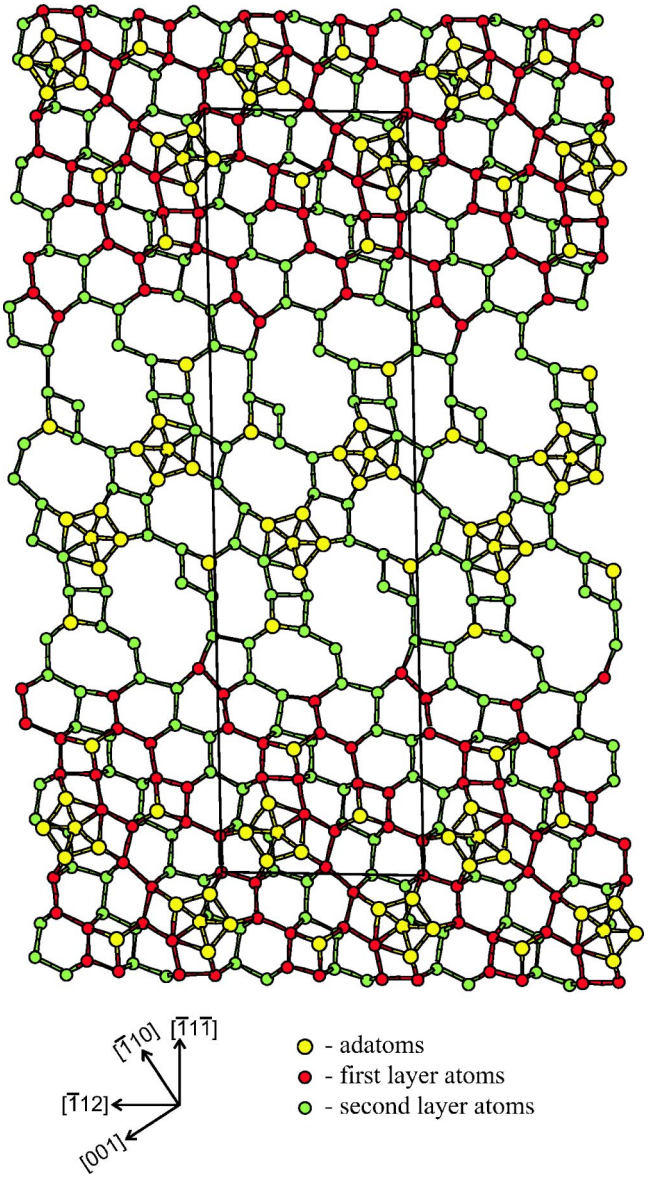

FIG. 8. (Color online) Top view of a possible 16×2 reconstruction. A unit cell is indicated.

IV. SUMMARY

Using *ab initio* calculations we have studied a variety of reconstructions of Si and Ge(110) surfaces with 1×1, 1×2, 2×1, $c(2\times2)$, 2×2, 3×1, 3×2, or 6×2 translational symmetry. Among the reconstruction elements are buckled zig-zag chains, adatoms, rest atoms, dimers, bridge-site atoms, pentamers, and interstitial atoms. In general neighboring chains buckled and laterally displaced in opposite directions and adatoms arranged along the [001] direction stabilize the (110) surfaces. For Ge adatom-rest atom pairs are the most stable reconstruction elements. In the case of Si the presence of only adatoms can lower the surface energy. Pure dimer structures and saturation of all dangling bonds by fourfold coordinated adatoms are not possible for both semiconductors. The tetramer-interstitial reconstruction is stabilized by additional adatoms. In this case the resulting pentamer atoms donate electrons to adatoms. Their dangling bonds are fully occupied what leads to a semiconducting band structure (at least for Si). Simulated empty-state STM images show pentagon-shaped spot distributions. The reconstruction element with two five-membered rings is completely unfavorable from the energetical point of view for both Si and Ge(110) surfaces, although this metastable structure can reproduce two pentagons in the empty-state STM images. Combining with other stable elements the adatom-tetramer-interstitial configuration may contribute to the stabilization of larger 16×2 or $c(8\times10)$ reconstructions of the Si and Ge surfaces. However, a definite answer can only be given by converged total-energy minimizations and STM simulations for $16\times2\,[c(8\times10)]$ reconstructed surfaces including the discussed reconstruction elements and surface steps or trenches. Nevertheless, we suggested a model for the 16×2 reconstruction in Fig. 8. Of course, it contains such elements as rebonded steps which have not been studied in the present paper.

ACKNOWLEDGMENTS

We acknowledge financial support from the Deutsche Forschungsgemeinschaft (Project No. Be1346/12-1) and the European Community in the framework of the Research and Training Network NANOPHASE (Contract No. HPRN-CT-2000-00167).

[1] D. J. Eaglesham, A. E. White, L. C. Feldman, N. Moriya, and D. C. Jacobson, Phys. Rev. Lett. **70**, 1643 (1993).
[2] F. Bechstedt, *Principles of Surface Physics* (Springer, Berlin, 2003).
[3] H. Ampo, S. Miura, K. Kato, Y. Ohkawa, and A. Tamura, Phys. Rev. B **34**, 2329 (1986).
[4] Y. Yamamoto, Phys. Rev. B **50**, 8534 (1994).
[5] Y. Yamamoto, T. Sueyoshi, T. Sato, and M. Iwatsuki, Surf. Sci. **466**, 183 (2000).
[6] T. An, M. Yoshimura, I. Ono, and K. Ueda, Phys. Rev. B **61**, 3006 (2000).
[7] B. A. Nesterenko, A. V. Brovii, and A. T. Sorokovykh, Surf. Sci. **171**, 495 (1986).
[8] E. J. van Loenen, D. Dijkkamp, and A. J. Hoeven, J. Microsc. **152**, 487 (1988).
[9] B. X. Olshanetsky, A. M. Kepinsky, and A. A. Shklyaev, Surf. Sci. **64**, 224 (1977).
[10] Z. Gai, R. G. Zhao, and W. S. Yang, Phys. Rev. B **57**, R6795 (1998).
[11] H. Noro and T. Ichikawa, Jpn. J. Appl. Phys., Part 1 **24**, 1288 (1985).
[12] T. Ichikawa, Surf. Sci. **544**, 58 (2003).
[13] A. I. Shkrebtii, C. M. Bertoni, R. Del Sole, and B. A. Nesterenko, Surf. Sci. **239**, 227 (1990).
[14] W. E. Packard and J. D. Dow, Phys. Rev. B **55**, 15 643 (1997).
[15] J. Dabrowski, H.-J. Müssig, and G. Wolff, Phys. Rev. Lett. **73**, 1660 (1994).
[16] M. Menon, N. N. Lathiotakis, and A. N. Andriotis, Phys. Rev. B **56**, 1412 (1997).
[17] N. Takeuchi, Surf. Sci. **494**, 21 (2001).
[18] A. A. Stekolnikov, J. Furthmüller, and F. Bechstedt, Phys. Rev. B **65**, 115318 (2002).
[19] P. Hohenberg and W. Kohn, Phys. Rev. **136**, B 864 (1964).
[20] W. Kohn and L. J. Sham, Phys. Rev. **140**, A 1133 (1965).
[21] J. P. Perdew and A. Zunger, Phys. Rev. B **23**, 5048 (1981).
[22] J. Furthmüller, P. Käckell, F. Bechstedt, and G. Kresse, Phys. Rev. B **61**, 4576 (2000).
[23] S. G. Louie, S. Froyen, and M. L. Cohen, Phys. Rev. B **26**, 1738 (1982).
[24] G. Kresse and J. Furthmüller, Comput. Mater. Sci. **6**, 15 (1996); G. Kresse Phys. Rev. B **54**, 11 169 (1996).
[25] M. S. Hybertsen and S. G. Louie, Phys. Rev. B **34**, 5390 (1986).
[26] F. Bechstedt, Adv. Solid State Phys. **32**, 161 (1992).
[27] J. Tersoff and D. R. Hamann, Phys. Rev. B **31**, 805 (1985).
[28] A. Cricenti, B. Nesterenko, P. Perfetti, and C. Sebenne, J. Vac. Sci. Technol. A **14**, 2448 (1996).
[29] A. A. Stekolnikov, J. Furthmüller, and F. Bechstedt, Phys. Rev. B **67**, 195332 (2003).